공학석사학위논문

Rheological investigation on different reactivity of polymer/clay nanocomposite to electric field

고분자/점토 나노복합체의 전기장에 대한 반응성 차이에 대한 유변학적 연구

2013년 8월

서울대학교 대학원

화학생물공학부

옥 현 근

Abstract

Rheological investigation on different reactivity of polymer/clay nanocomposite to electric field

Ock, Hyun Geun
School of Chemical and Biological Engineering
The Graduate School
Seoul National University

In this study, the A.C. electric field effect was investigated according to combination of polymer/clay nancomposite. Nonpolar polypropylene and polar poly(lactic acid) were used as two base polymers. Three organically modified clays(Closite 10A, 20A, 30B) were chosen based on the structural difference of modifiers. Polymer/clay nanocomposite was produced by melt compounding. The A.C. electric field was applied during dynamic time sweep test on the modified fixture of RMS using a function generator and high voltage amplifier. The electric field effect was first confirmed by storage modulus change in dynamic time sweep test. The storage modulus of each polymer/clay nanocomposite was increased with time and both the increment and the magnitude of final value were dependent upon the activated electric field strength. The frequency sweep test was conducted before and after electric field was activated. The storage modulus at low frequency was highly increased with applied electric field strength and terminal slope approached to near zero. The reactivity to electric field was very different in terms of each combination of polymer/clay nanocomposite. To quantify the extent of electrical reactivity, normalized storage modulus was regressed using universal exponential rising equation. The fitted result showed that the electrical reactivity was decided at the initial state of the reaction, so the initial tangential slope of normalized modulus was suggested to represent the reactivity to the electric field. In case of

polypropylene/clay, the reactivity was in the order of C20A, C10A and C30B, while poly (lactic acid)/clay showed the opposite order, followed by C30B, C10A and C20A. The electrical reactivity was dependent structural similarity between polymer and clay, so Hansen solubility parameter was introduced to express this structural affinity. Polymer/clay combination, which shows similar Hansen solubility parameter, was highly reactive to electric field.

Key words: Rheology, polymer nanocomposite, electric field, organoclay, polypropylene, poly (lactic acid)

Student Number: 2011-21049

Contents

List of Figures

List of Tables

Chapter 1 Introduction

1.1 Polymer/clay nanocomposite

Polymer nanocomposite is composed of organic base polymer and inorganic nanoparticles. It is being highly magnified as a as high performance hybrid material which could be used in many industrial fields, arising from light weight, nano-sized scale and large surface area.

Especially, there have been many researches about polymer/clay nanocomposite expecting to enhance both permeability from its layered structure and mechanical, thermal properties of polymer attributed from high aspect ratio of layered silicates. Moreover, it is greatly expected to enhance various physical properties of polymer compared to conventional micro-sized inorganic filler just with small weight fraction of nanoclay, originated from its nano-scale size. As a result, it is essential to get well dispersed structures of each layered silicate for nano size effect of clay. It is known that the nanoclay is composed of stacked structures of many layered silicate by very strong Van der Waals attractive force between each platelet in nature [1]. Therefore, the distance between each silicate layers should be widened to get well-dispersed state of nanoclay, which is called exfoliation. It is suggested that clay could be exfoliated by following two steps. The first step is penetration of polymer chain into widened gap between clay platelet and the second step is separation of each silicate layer [2]. Since well-exfoliated state is directly related to physical properties of polymer/clay nanocomposite system, there have been many researches to get exfoliated structures of nanoclay in polymer matrix.

1.2 Nanoclay exfoliation methods

The exfoliation methods of nanoclay could be classified as chemical and physical approaches, generally. There are many types of chemical approaches, which are solution casting, in-situ polymerization and clay modification methods [3]. These chemical methods are focusing on changing compatibility between organic polymer and inorganic nanoclay by modifying structures of materials or using additional agents like catalyst or functional group in processing steps of nanocomposite or synthesizing steps of clay particle. In terms of nanoclay particle, the structure of clay is basically hydrophilic but it is possible to control its hydrophilicity by substituting different desired organic functional groups from cationic exchange. The nanoclay which is functionalized with organic modifiers is so called organoclay. Among many types of clay in nature, montmorillonite is being widely used because of its high ion exchangeable ability. The surface of pristine montmorillonite could be substituted by organic modifier and it is called organic modified montmorillonite (OMMT). The modifier of OMMT could be designed to give selective compatibility to a specific polymer matrix, so this functionalizing method of nanoclay is one of the most useful ways to exfoliate clay particle in matrices. Graft copolymer which has more hydrophilic functional groups is also another chemical approach as a compatibilizer for hydrophobic polymer with the same purpose of OMMT. However, it is difficult to find suitable compatibilizer for many polymers and the used copolymer might decrease original physical properties of pristine polymer. On the other hand, physical approach for clay exfoliation is to apply strong extra force to separate silicate layers and high shear force, U.V. magnetic field, electric field could be used.

1.3 Biodegradable polymer/clay nanocomposite

One of the polymers used in the study, poly (lactic acid) is a biodegradable polymer, which is derived from separating starches from corn or synthesized from different bio-resourced materials. Many researches about poly (lactic acid) are being investigated to solve the problems of non-degradability of plastic products. Since PLA has low thermal stability and poor mechanical property, it is restricted to apply PLA to many industrial applications. PLA/clay nanocomposite could be an answer for this problem [3, 4]. The thermal, mechanical and rheological property would be improved with well dispersed structures of clay [5, 6]. The structures of many biodegradable polymers have hydrophilic functional group and it could give compatibility with inorganic clay particles. It would be very assistive to make exfoliated nanocomposite with respect to the polarity of nanoclay. In this study, the electric field effect for clay dispersion in PLA/clay nanocomposite was investigated for effective use of PLA [7].

1.4 Electric field to fabricate polymer/clay nanocomposite

The chemical approaches for clay exfoliation is limited to apply for the real industrial field, so physical method is getting investigated. In 2003, Kim et al introduced the electric field as a tool for fabricating polymer/clay nanocomposite in Fig. 1.1 [8]. He insisted that the A.C. electric was more effective than the D.C. electric field in case of polypropylene/clay nanocomposite. The electric field effect for exfoliation of clay was examined by XRD, TEM and rheological analysis. In SAXS measurement, distance between clay platelet became widened, while oscillating under the A.C. electric field. On the other hand, the distance was shortly broadened at the first time showing just modest change in overall reaction [9]. From observation of dielectric properties, it was detected that bound ions around clay surface was decreased with activated A.C. electric field duration time. Based on the result, it was insisted that the A.C. electric field caused change of surface charge distribution, which meant decrease of the Van der Waals attractive force between clay platelets.

In this regard, when the electrostatic repulsion overcomes Van der Waals interaction by the applied A.C. electric field, the gallery between clay platelets would become widened. Polymer chain would move toward clay platelets and the affinity between polymer and clay would be the governing factor. The objective of the study is to investigate structural development of polymer/clay nanocomposite, in terms of affinities between polymer and clay. For the purpose of the objective, a non-polar polypropylene and a polar poly (lactic acid) as base polymers and three different types of organoclay as particles were used to confirm the effect of polarity of polymers for electric field effect.

Chapter 2 Experimental part

2.1 Materials

Polypropylene (HP-740T, melt flow rate 60g/10min, at 230℃/2.16kg) was supplied by Polymirae Company Ltd and poly (lactic acid) (4032D, melt flow rate 1.0g/10min, at 200℃/2.16kg) were provided by Nature Works Co. Ltd. Three commercial different types of organically modified clay (Closite 10A, 20A, 30B) from Southern Clay Products, Inc. were used. The information of structures and characteristics of organoclay used in the study are listed in table 1.

2.2 Sample preparation

All the samples were dried in the vacuum over at 80 for 8 hours before compounding. After drying samples, polymer/clay nanocomposite was prepared by melt compounding using an intensive internal batch mixer (Hakke, Rheomix 600 & rheocord 90). The weight fraction of each organoclay was fixed at five weight percent. Polymer was first put into the mixer and then five weight percent of nanoclay was inserted after one minute of stabilizing step of polymer to be melted. The rotor speed was continued at 100rpm for 8 minutes after organoclay was fed. The processing temperature of 190℃ for PP and 210℃ for PLA, respectively. For rheological measurement and morphology observation, compounded nanocomposites were molded into disk shape of 25mm diameter and 1mm thickness.

Table 1. Information and characteristic of organoclay used in the study

Notation	Tradename	Characteristics
C20A	Cloisite®20A	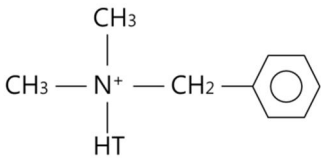 HT : Hydrogenated Tallow (~65% C18; ~30% C16; ~5% C14)
C10A	Cloisite®10A	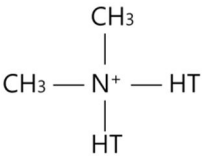
C30B	Cloisite®30B	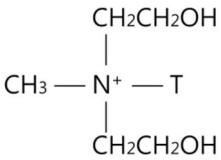 T : Tallow (~65% C18; ~30% C16; ~5% C14)

2.3 Electric field activation

To activate electric field on polymer nanocomposite, a pair of 25mm parallel plate fixture for RMS was modified. The upper part of the fixture was consisted of steel for electric field activation. The central part of the fixture was made by PEEK (poly-ether-ether-ketone) to be insulated from generated current. The electric field was applied on a rheometer, while conducting dynamic time sweep test at frequency 1rad/s and under linear strain range after the maximum linear strain was confirmed by conducting dynamic strain sweep test at frequency 1 and 100 rad/s. The electric power was generated by a function generator (AFG310, Tektronix, USA) and the A.C. electric field was amplified using a high voltage amplifier (677B, Trek, USA) with 60Hz frequency and different electric field strength (325, 550, 775, 1000V/mm). The applied voltage was confirmed by a digital oscilloscope (TDS210, Tektronix, USA).

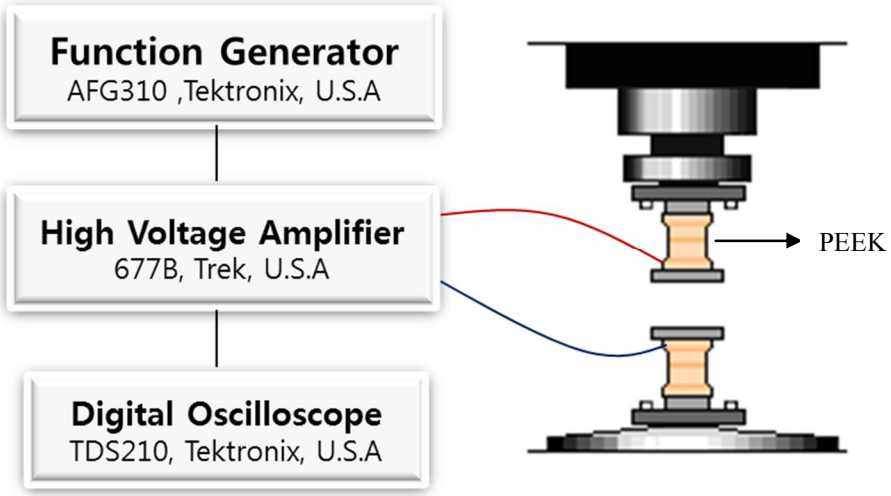

Figure 2.1 Schematic of modified fixture for RMS and tools for activating electric field

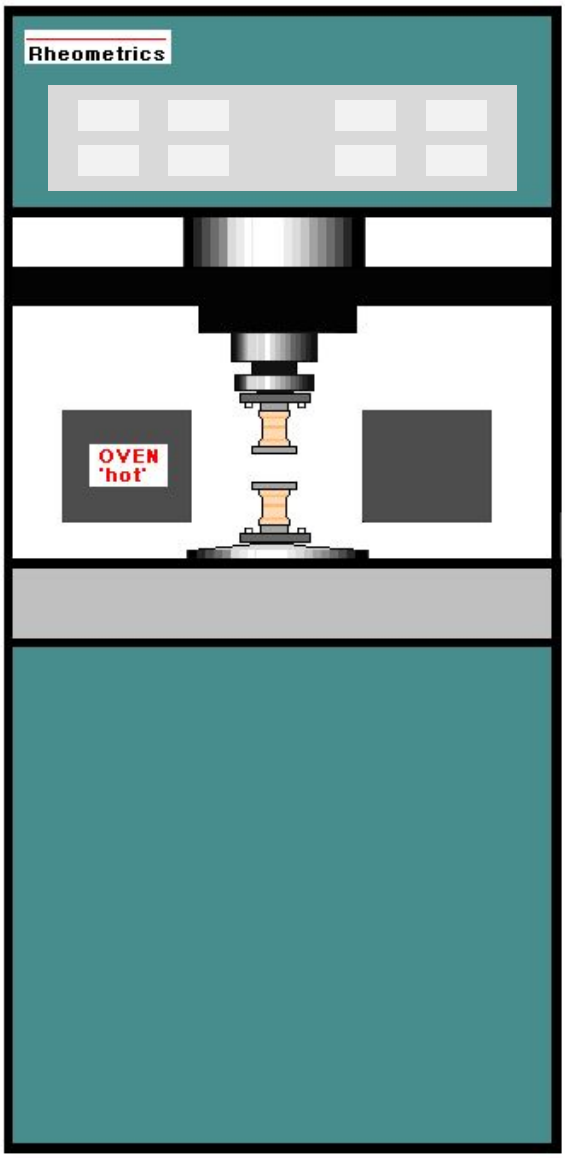

Figure 2.2 Schematic of modified fixture on RMS-800

2.4 Characterization

2.4.1 Dynamic time sweep test

Rheological measurement was conducted using strain-controlled Rheometrics Mechanical Spectrometer (RMS-800), while measuring temperature was 170℃ for PP and 190℃ for PLA. Dynamic time sweep test was performed at linear strain range, frequency 1rad/s. For the first two minutes, time sweep was carried out with no electric field activation for stabilizing time. The electric field was applied after duration time and the field kept to be activated at the end of the test.

2.4.2 Dynamic frequency sweep test

Dynamic frequency sweep test was carried out using 25mm diameter and 1mm thick modified fixture in linear strain region of each sample at frequency range of 0.1~100 rad/s, before and after electrical treatment. The measuring temperature was 170℃ for PP and 190℃ for PLA, same with the time sweep test. The measuring was performed after half cycle delay.

2.4.3 Transmission Electron Microscopy morphology

Transmission Electron Microscopy (TEM) morphology of each electrically treated polymer/clay nanocomposite was observed by JEOL 2100F at an acceleration voltage of 200kV. Each sample was taken by cryo-sectioning in nitrogen atmosphere using PT PC Ultramicrotome.

Chapter 3 Results and discussion

3.1 Electric field effect on polymer/clay nanocomposite

3.1.1 Microstructural development of PP/clay and PLA/clay nanocomposites under the A.C. electric field

As a first step of the study, the electric field effect on clay exfoliation in polypropylene matrix was investigated by rheology and morphology. Fig. 3.1 shows dynamic time sweep results of PP/C20A nanocomposite under each electric field strength (325, 550, 775, 1000V/mm). The A.C. electric field was applied after two minutes duration time. The storage modulus of PP/C20A composite was increased with electric field activating time once the A.C. field was applied, showing microstructural development, which is similar with typical gelation or networking structure forming reaction [10]. It could be explained that this microstructural evolution of PP/C20A nanocomposite was caused exfoliation of clay under the electric field. The modulus at each of electric field strength continuously rose for about 10 minutes and became saturated. Also, the saturated value of storage modulus under each electric field was increased with the magnitude of the applied electric field strength. The storage modulus change of PLA/C30B nanocomposite in Fig. 3.2 also showed similar behavior with PP/C20A nanocomposite.

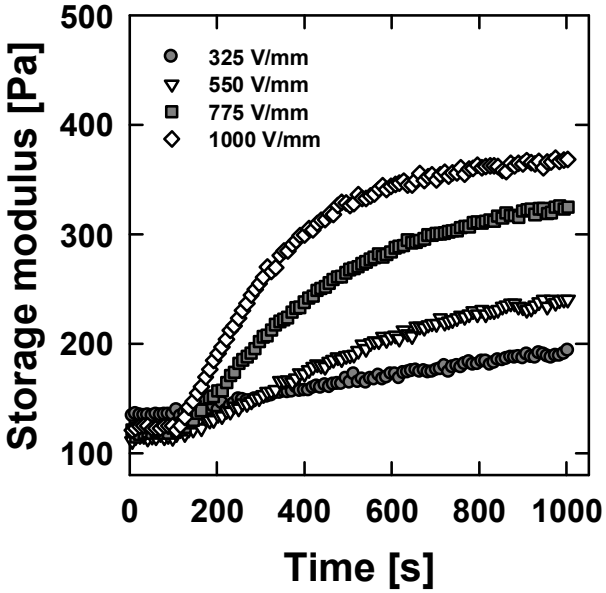

Figure 3.1 Dynamic time sweep result under each electric field strength (325, 550, 775, 1000V/mm) of polypropylene/C20A nanocomposite

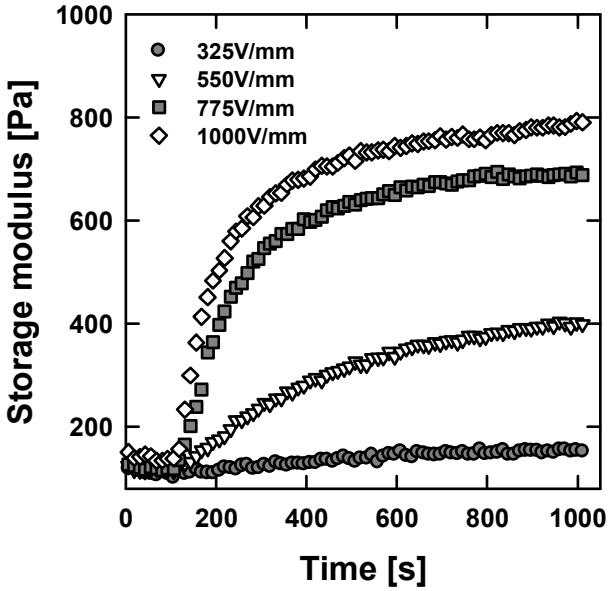

Figure 3.2 Dynamic time sweep result under each electric field strength (325, 550, 775, 1000V/mm) of poly (lactic acid)/C30B nanocomposite

3.1.2 Dynamic frequency sweep test

The dynamic frequency sweep test after electrical treatment was conducted to confirm structural development of PP/C20A nanocomposoite in Fig. 3.3. The storage modulus at low frequency increased depending upon electric field strength. Also, the terminal slope of the moduli approached to near zero, which suggested liquid to pseudo-solid like transition of PP/C20A composite by the electric field [11, 12]. The storage moduli at 0.1 rad/s and terminal slope under different electric field strength was listed in table 2. PLA/clay nanocomposites also showed similar behavior with PP/C20A in the frequency sweep test in Fig. 3.4. However, the increment of the modulus of PLA/C30B composite was two times higher than PP/C20A composite. It could be explained that the reactivity to electric field of PLA/C30B combination is much higher, showing more efficient effect of the electric field. This different of reactivity to the electric field would be discussed later.

In order to observe these micro-structural change with the magnitude of electric field strength, Transmission Electron Microscopy morphology from was taken.

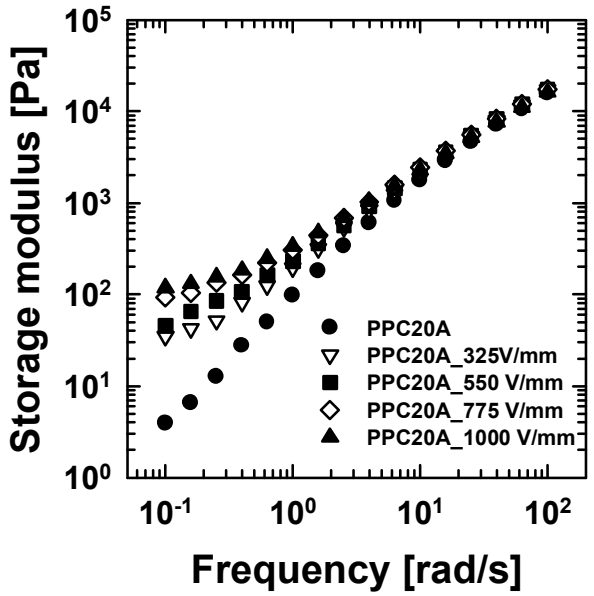

Figure 3.3 Frequency sweep result after the electric field was activated strength (0, 325, 550, 775, 1000V/mm) of PP/C20 nanocomposite

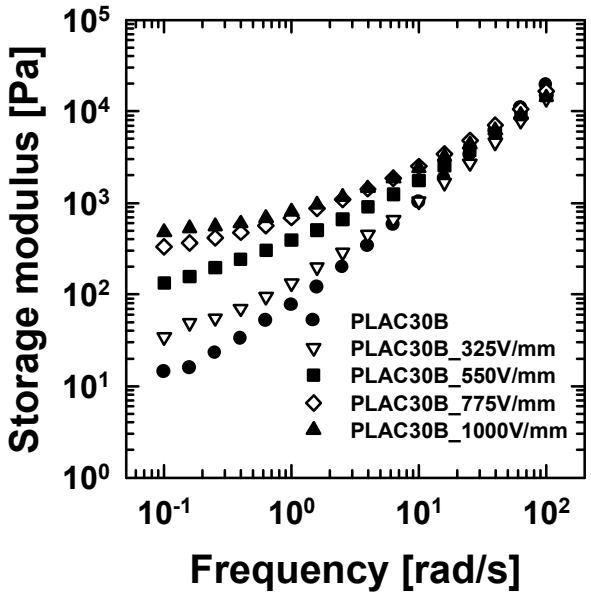

Figure 3.4 Frequency sweep result after the electric field was activated strength (0, 325, 550, 775, 1000V/mm) of PLA/C30B nanocomposite

Table 2 Terminal slope and storage modulus at 0.1 rad/s of PP/C20A under each applied electric field strength (0, 325, 550, 775, 1000V/mm)

	0V/mm	325V/mm	550V/mm	775V/mm	1000V/mm
G' at 0.1 rad/s	2.54	35.1	45.2	92.9	119
Terminal slope	1.41	0.71	0.62	0.42	0.32

3.1.3 TEM microscopy morphology

In Fig 3.5, TEM images of PP/C20A nanocomposite could give similar analysis with rheological properties of it. As an electric field increased, layer-stacking of clay tactoids destructed and layered silicate was separated. The result implies that the A.C. electric field made clay particles to be exfoliated. In case of PLA/C30B nanocomposite, the morphological change with electric field strength was similar with that of PP/C20A nanocomposite in Fig 3.6. From these results – rheological data and TEM morphology, it can be inferred that clay is dispersed in polypropylene melt by activating electric field.

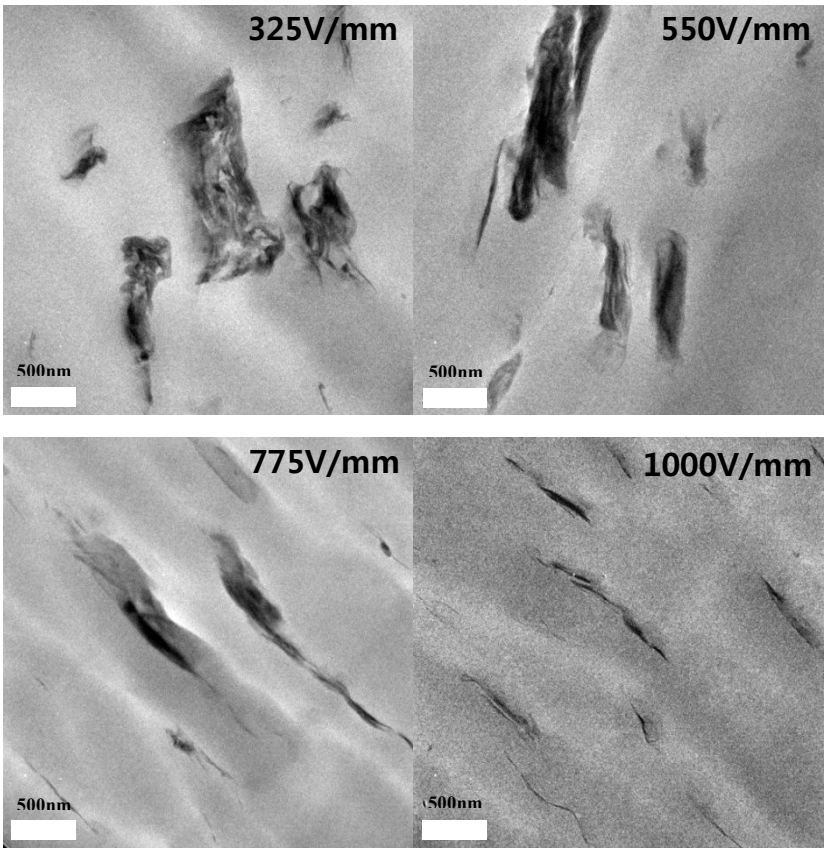

Figure 3.5 TEM morphology of PP/C20A nanocomposite after the A.C. electric field was activated (325, 550, 775, 1000V/mm)

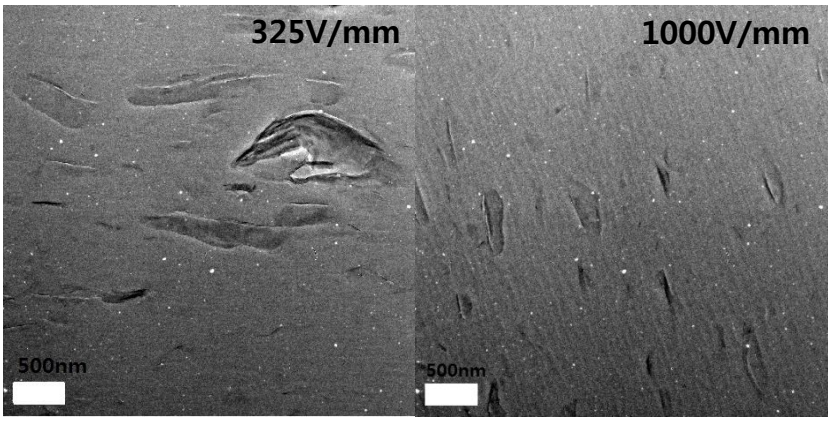

Figure 3.6 TEM morphology of PLA/C30B nanocomposite after the A.C. electric field was activated (325, 1000V/mm)

3.2 Quantification of electrical reactivity

3.2.1 Non-linear regression using mathematical equation

The storage modulus of each nanocomposite was normalized to fit the initial modulus in order to compare each combinations of nanocopmosite. Park et al suggested that storage modulus of polypropylene/clay nanocomposite with time could be fitted by universal exponential rise equation of one parameter function in equation 1 [13].

$$\frac{G'(t)-G'_0}{G'_i-G'_0} = 1 - \exp(-\frac{t}{\lambda}) \qquad (1)$$

The slope of exponential function of PLA/clay, which represents the reactivity to electric field, is too much higher than that of PP/clay composite. As a result, equation 1 didn't trace the storage modulus curve of each nanocomposite, properly. Here, the same equation was modified as two parameter function to track the modulus curve more accurately.

$$\frac{G'(t)}{G'_0} = 1 + a(1 - \exp\left(-\frac{t}{\lambda}\right)) \qquad (2)$$

The curve of the normalized storage modulus of each polymer/clay nanocomposite was fitted by the universal exponential rising equation. The storage modulus of PP/C20A and PLA/C30B composite with time were shown in Fig 3.7, respectively.

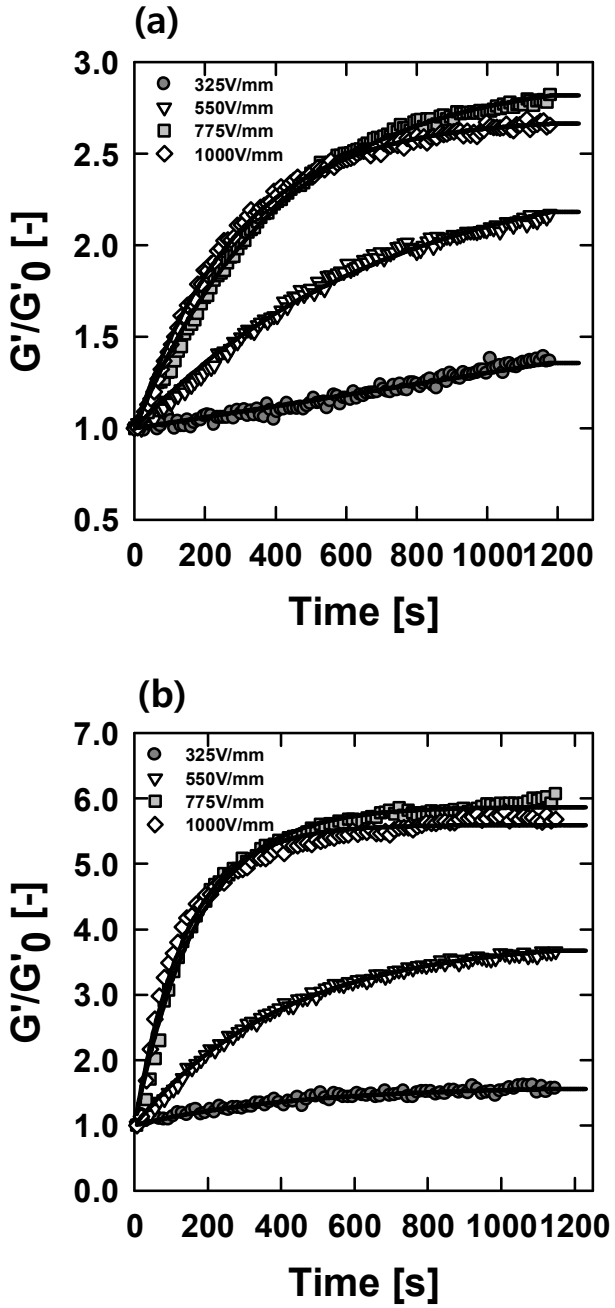

Figure 3.7 Fitted normalized storage modulus under the A.C. electric field with time (a) PP/C20A (b) PLA/C30B nanocomposites

3.2.2 Parameters representing electrical reactivity

From the equation 2, parameter a represent how fast the modulus increases and parameter λ signifies the final value of the modulus. So, both of two parameters a and λ could express the electrical reactivity, reasonably. However, the degree of electrical response at the higher electric field strength, i.e. 775, 1000V/mm was shown as fully saturated and the final value was no more dependent on the applied electric field strength. A new parameter a λ, which is the initial tangential slope of the exponential curve, was suggested as a new parameter to represent the reactivity to electric field of each polymer/clay nanocomposite. It would be called as the initial rate. Fig. 3.8 shows fitted initial tangential slope of storage modulus with time of each nanocomposite.

The initial rate of each material was plotted with electric field strength in Fig. 3.9. The initial rate first increased with electric field strength and then became saturated after about 10 minutes. The initial rate of polypropylene/clay was in the order of C20A, C10A and C30B, while the initial rate of poly (lactic acid)/clay showed the opposite order. The curve of the initial rate with electric field strength was exponential rising shape, which is very similar with storage modulus curve with time. So, it could be said that it is quite reasonable to use the initial rate as a representative for the reactivity to electric field of each polymer/clay nanocomposite.

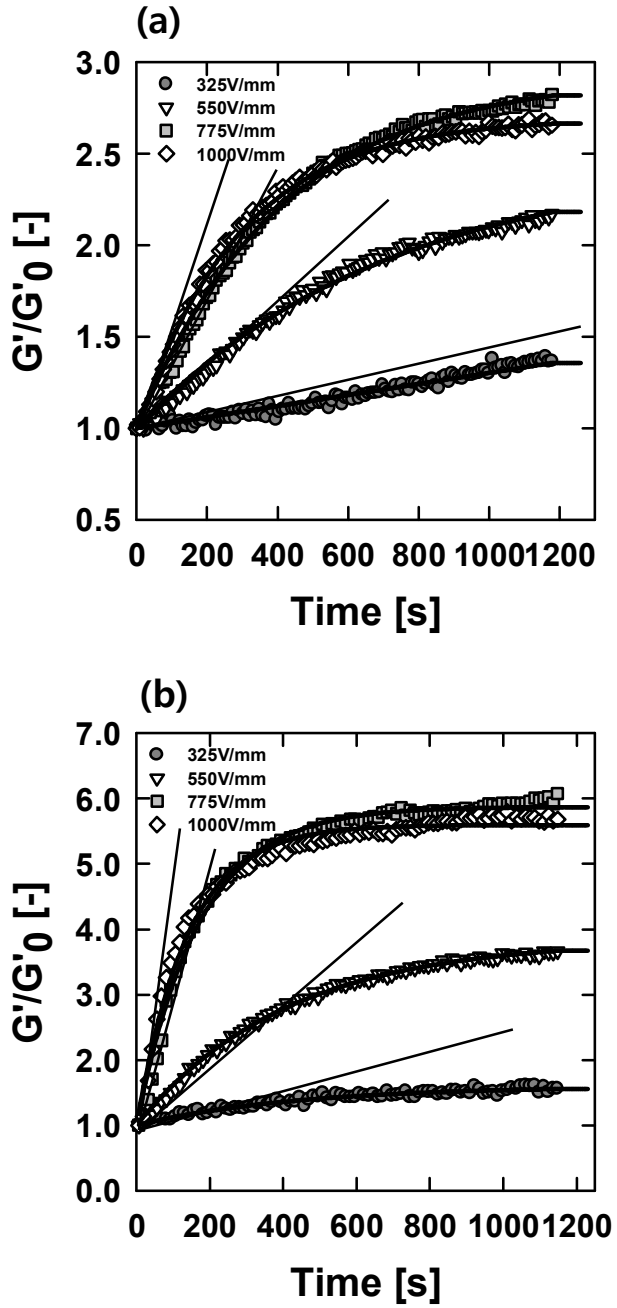

Figure 3.8 Initial tangential slope of fitted normalized storage modulus under the A.C. electric field with time (a) PP/C20A (b) PLA/C30B nanocomposites

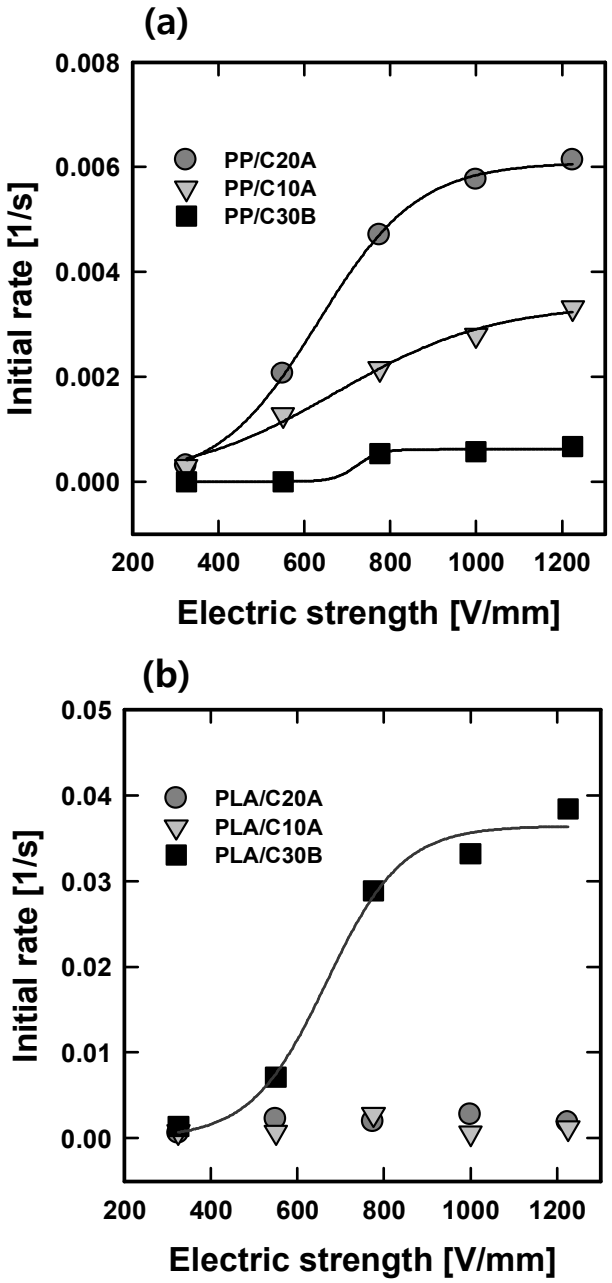

Figure 3.9 Initial growth rate as a representative for reactivity to the electric field (a) polypropylene/clay (b) poly (lactic acid)/clay nanocomposites

3.2.3 Time-electric field superposition

Park et al suggested that the electric field strength and the field activating time are equivalent each other from time-electric field superposition. He proposed that each storage modulus under both D.C. and A.C. could be superposed making universal master curve by shifting characteristic time λ from equation 1 [15]. However, the electrical reactivity depending on different base polymer didn't be superposed by equation 1, since the reactivity of PP and PLA to the electric field was too distinct from one another. Even in case of nanocomposite with same base polymer and different clay, the electric reactivity shows too much difference. Instead, the two parameter equation was used to superpose each electrical response, where parameter a is relevant to vertical shift factor and parameter λ is for horizontal shift factor. The result shows that the master curves of each storage modulus under the electric field of polymer/clay nanocomposite were superposed well, except for several cases whose electrical response was too low to be detectable in Fig. 3.10 and 3.11.

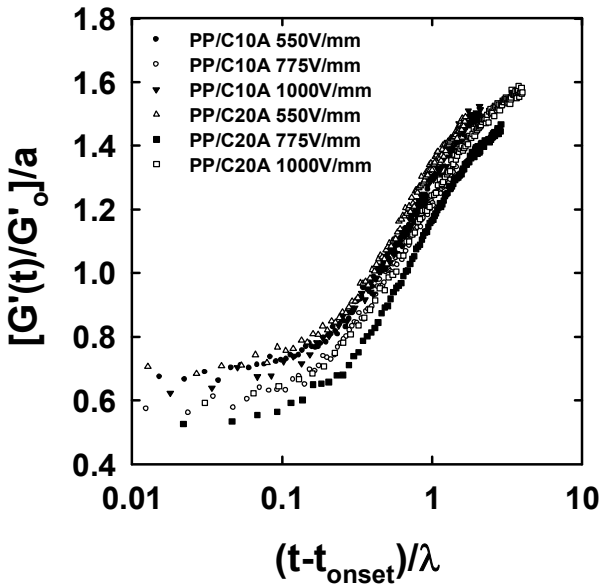

Figure 3.10 Master curve of PP/clay nanocomposites by time-electric field superposition

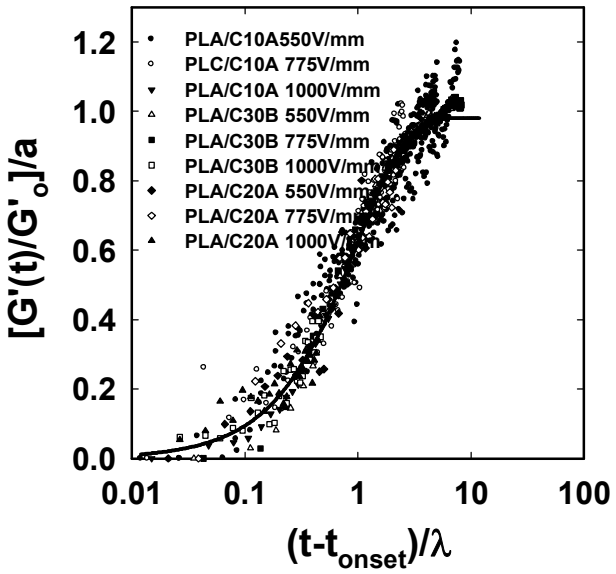

Figure 3.11 Master curve of PLA/clay nanocomposites by time-electric field superposition

3.3 Comparison of electrical reactivity of polypropylene/clay with poly (lactic acid)/clay nanocomposite

3.3.1 Different reactivity to the electric field of each PP/clay and PLA/clay combinations

The extent of electrical reactivity of PP/clay nanocomposite was shown in the order of PP/C20A, PP/C10A and PP/C30B. In case of PP/C30B and PP/C10A nanocomposite in Fig. 3.12, the electric field was less effective than PP/C20A combination. In the previous research, it was suggested that role of the A.C. electric field is to make clay platelet to be widened due to the increased electrostatic repulsive force by electric field. It was insisted that these different reactivity to electric field was dominated by distance between gallery, while the distance of C20A showed the higher value followed by C30B, C10A. However, this explanation is not matched to the reactivity of PLA/clay nanocomposite. The response to electric field of PLA/clay nanocomposite was shown in the sequence of C30B > C10A > C20A. This result suggests that there existed another step of the A.C. electric field for clay exfoliation except the first step. Again, the first step is that gallery between clay platelets becomes widened. The possible second step is that polymer chain moves toward widened gallery, resulting to accelerate exfoliation of clays. As a result, the different reactivity of each polymer/clay nanocomposite to electric field is decided by polymer mobility.

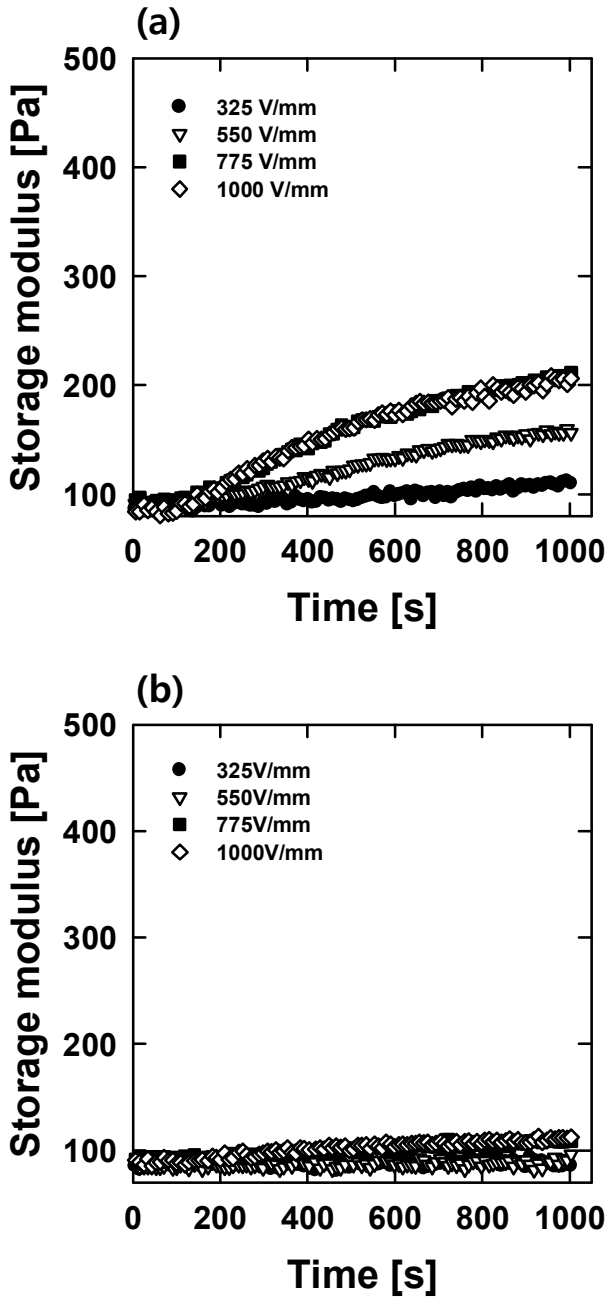

Figure 3.12 Time sweep result of (a) PP/C10A (b) PP/C30B nanocomposites under each electric field strength (325, 550, 775, 1000V/mm)

3.3.2 Structural similarity between base polymer and organoclay

There are many variables which affects polymer chain mobility like temperature, weight fraction of polymer and molecular weight and so on [14]. However, it could be regarded that in the confined system in which those parameters were fixed, the main driving force would be intermolecular interactive force, i.e. Dipole-dipole interaction, Van der Waals force, Hydrogen bonding. Under the electric field, the main element to make polymer move toward gallery between clay platelet could be affinities between polymer and clay [15]. In terms of structures of each material, it could be considered this different tendency of the reactivity to electric field could be explained by structural similarity between polymer and clay.

When it comes to the structures of modifiers of nanoclays, it could be possibly understood that the most effective clay for each polymer has very similar structure with each polymer. For example, C30B is composed of one tallow (long tail hydrocarbon, C14~C18), methyl group and 2-hydroxyethyl groups around a quaternary ammonium ion. Since the role of tallow is to spread the distance between layered silicates, surface feature of nanoclay is decided by the other functional groups except tallow. The predominant elements which determine functionality of C30B are methyl and 2-hydroxyethyl groups. The surface property of C30B shows high electronegative structure due to two unpaired electrons near oxygen atom and it is possible for polar PLA to interact with it by hydrogen bonding.

On the other hand, with respect to C20A which is consisted of two hydrogenated tallow and dimethyl groups, the dominate functional group is methyl group whose structure is almost non-polar. Consequently, the C20A tends to connect to polymer by induced dipole-induced dipole interaction

(Van der Waals interactive force). Therefore, it would strongly interact with polypropylene than poly (lactic acid). The other clay used in the study is C10A, that is made up with one hydrogenated tallow, dimethyl and benzyl group. The structure of C10A has in-between polarity compared with C20A and C30B. As a result, the C10A would show intermediate reactivity with both polypropylene and poly (lactic acid).

It is known that polymer chain moves toward clay platelets in intercalation process and makes clay to be exfoliated [16]. It could be suggested that there were two possible steps of the electric field for clay exfoliation similar with typical exfoliation mechanisms of clay. Under the electric field activated condition, polarization of polymer is also to be accelerated, resulting to get high intermolecular interactive potential. When the A.C. electric field was applied to the polypropylene/clay nanocomposites, polypropylene chain could move toward to galleries of clay platelet.

In accordance with the molecular structures of polymer and organic modifiers of nanoclay, the structures of polypropylene and the organic modifier of C20A are most similar out of many combinations of polymer nanocomposite, while those of poly (lactic acid) and C30B are most similar combination.

3.4 Explanation of different reactivity of each nanocomposite

3.4.1 Introduction of Hansen Solubility parameters

Based on the correlation between different reactivity to the electric field and structural similarity between polymer and clay, it could be regarded that the electrical reactivity of polymer/clay nanocomposite was dependent upon affinities between base polymer and the functional group of clays. In order to express the correlation between the structural similarity and the electrical reactivity, solubility parameter was introduced [17].

Solubility parameter is used to estimate miscibility of materials. It is known that polymer would dissolve in a solvent whose solubility parameters are similar to its own. In general case, the solubility parameters represent structural similarity and affinities between two materials and it could be applied to explain the affinities between base polymer and nanoparticle in polymer nanocomposites [18]. There are several kinds of solubility parameters but most of them are derived from cohesive energy density based on the structures of materials. In this study, Hansen Solubility Parameter (HSP) was used to explain different response of polymer nanocomposites to electric field. The total solubility parameter (δ) is derived from dispersion (δ_d), polar interaction (δ_p) and hydrogen-bonding (δ_h) terms, where F is attraction constant, U in internal energy and V is Van der Waals volume.

$$\delta_d = (\sum_z (F_d)_z)/V \qquad \delta_p = \left(\sum_z \left(F_p\right)_z^2\right)^{\frac{1}{2}}/V \qquad \delta_h = (\sum_z - U_z/V)^{\frac{1}{2}} \qquad (2)$$

$$\delta = \left(\delta_d^2 + \delta_p^2 + \delta_h^2\right) \qquad (3)$$

3.4.2 Correlation between Hansen Solubility Parameter and electrical reactivity

The Hansen solubility parameter of each polymer and the organic modifier of clay were calculated using following equations from references in table [19, 20]. The magnitude of calculated Hansen solubility parameters are in the sequence of PLA > C30B > C10A > C20A > PP. It is known that the less difference between solubility parameters of two materials, the more compatible they are. Based on the calculated value, compatibility between polymer and organic modifiers of clay could be predicted. Polypropylene would be most compatible with C20A followed by C10A and C30B. In contrast, the compatibility of clay with poly (lactic acid) would be in the order of C30B, C10A and C20A.

Polypropylene and C20A have nearly the same HSP value, while the value of PLA and C30B are similar. This result corresponds to the structural affinities of materials. Two materials which have similar solubility parameter mean that their structures are similar and they have affinities each other. Based on the functional groups of each material in Fig 3.13, the structures of PP and organic modifier of C20A are similar and those of PLA and modifier of C30B are also similar. The Hansen parameters are well matched to the results of different initial rates of each polymer/clay combinations in fig 3.6.

In conclusion, it could be understood that the affinities between polymer and clay was predominant factor to affect the reactivity to electric field of polymer/clay nanocomposite.

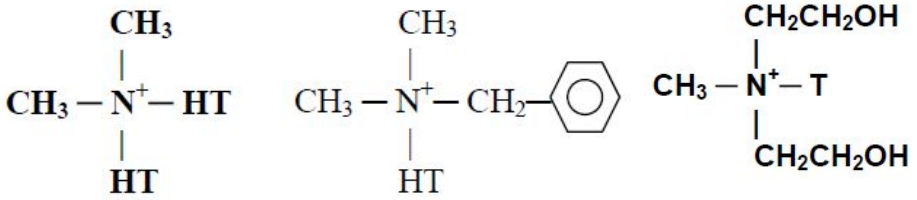

C20A C10A C30B

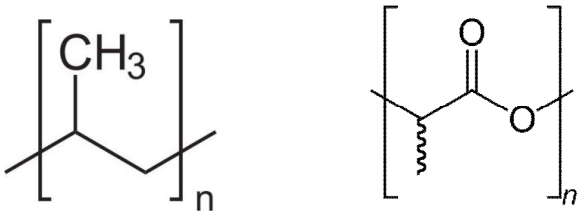

Polypropylene Poly(lactic acid)

Figure 3.13 Schematics of the structures of materials used in the study

Table 3. Information and characteristic of organoclay used in the study

	Dispersion (δ_d)	Polar interaction(δ_p)	Hydrogen bonding(δ_h)	Total solubility parameter(δ_t)
PP	15.8	0	0	15.8
PLA	15.7	18.4	10.3	26.3
C10A	19.1	2.3	5.5	20.0
C20A	16.9	1.5	5.2	17.7
C30B	21.6	3.2	10.9	24.4

Chapter 4 Conclusion

In this study, the A.C. electric field effect for fabricating polymer/clay nanocomposite was investigated. The electric field effect for clay exfoliation was first confirmed by dynamic time sweep test. The storage modulus increased with time approaching to steady value in a few minutes. In the dynamic frequency sweep test, the storage modulus of electrically activated polymer nanocomposite highly increased at low frequency and the terminal behavior went to be disappeared with applied electric field strength. TEM morphology showed that layer stacking was destructed and layered silicates were separated after electrical treatment. This structural development was caused by clay exfoliation and the extent of reactivity to electric field was higher in case of polymer/clay nanocomposite, whose structures were similar each other. The electrical reactivity was expressed by initial tangential slope of normalized storage modulus in time sweep test. Hansen solubility parameter was used to represent structural similarity between materials. The electric field was more effective for the polymer/clay nanocomposite, which showed similar Hansen solubility parameter. The most reactive combinations to electric field were PP/C20A and PLA/C30B nanocomposites whose structures were similar each other. The result showed compatibility between polymer and clay make important role to decide the reactivity to electric field of polymer/clay nanocomposite.

In conclusion, this correlation between structural similarity and reactivity to electric field could be expected by calculating Hansen solubility parameter, which could contribute to efficient use of the electric field for polymer/clay nanocomposite fabrication.

References

1. Pavlidou, S. and C.D. Papaspyrides, *A review on polymer–layered silicate nanocomposites.* Progress in Polymer Science, 2008. **33**(12): p. 1119-1198.
2. LeBaron, P.C., *Polymer-layered silicate nanocomposites an overview.* Applied Clay Science, 1999. **15**: p. 11-29.
3. Wu, D., et al., *Rheology and thermal stability of polylactide/clay nanocomposites.* Polymer Degradation and Stability, 2006. **91**(12): p. 3149-3155.
4. Sinha Ray, S., et al., *New Polylactide/Layered Silicate Nanocomposites. 1. Preparation, Characterization, and Properties.* Macromolecules, 2002. **35**(8): p. 3104-3110.
5. Di, Y., et al., *Poly(lactic acid)/organoclay nanocomposites: Thermal, rheological properties and foam processing.* Journal of Polymer Science Part B: Polymer Physics, 2005. **43**(6): p. 689-698.
6. Chow, W. and S. Lok, *Thermal properties of poly(lactic acid)/organo-montmorillonite nanocomposites.* Journal of Thermal Analysis and Calorimetry, 2009. **95**(2): p. 627-632.
7. David, H., et al., *Polylactic Acid Technology*, in *Natural Fibers, Biopolymers, and Biocomposites*. 2005, CRC Press.
8. Kim, D.H., et al., *Electrically Activated Poly(propylene)/Clay Nanocomposites.* Macromolecular Rapid Communications, 2003. **24**(5-6): p. 388-391.
9. Kim, D.H., et al., *Microstructural evolution of electrically activated polypropylene/layered silicate nanocomposites investigated by in situ synchrotron wide-angle X-ray scattering and dielectric relaxation analysis.* Polymer, 2006. **47**(16): p. 5938-5945.
10. Krishnamoorti, R., *Rheology of polymer layered silicate nanocomposites.* Current Opinion in Colloid & Interface Science, 2001. **6**: p. 464-470.
11. Reichert, P., et al., *Morphological stability of poly (propylene) nanocomposites.* Macromolecular rapid communications, 2001. **22**(7): p. 519-523.
12. Krishnamoorti, R. and R.A. Vaia, *Polymer nanocomposites.* Journal of Polymer Science Part B: Polymer Physics, 2007. **45**(24): p. 3252-3256.

13. Park, J.U., et al., *Time–electric field superposition in electrically activated polypropylene/layered silicate nanocomposites.* Polymer, 2006. **47**(14): p. 5145-5153.
14. Rastogi, S., et al., *Chain mobility in polymer systems: on the borderline between solid and melt. 1. Lamellar doubling during annealing of polyethylene.* Macromolecules, 1997. **30**(25): p. 7880-7889.
15. Gorman, W.G. and G.D. Hall, *Dielectric constant correlations with solubility and solubility parameters.* Journal of Pharmaceutical Sciences, 1964. **53**(9): p. 1017-1020.
16. Lan, T., P.D. Kaviratna, and T.J. Pinnavaia, *Mechanism of Clay Tactoid Exfoliation in Epoxy-Clay Nanocomposites.* Chemistry of Materials, 1995. **7**(11): p. 2144-2150.
17. Hansen, C.M., *The universality of the solubility parameter.* Industrial & Engineering Chemistry Product Research and Development, 1969. **8**(1): p. 2-11.
18. Jang, B.N., D. Wang, and C.A. Wilkie, *Relationship between the solubility parameter of polymers and the clay dispersion in polymer/clay nanocomposites and the role of the surfactant.* Macromolecules, 2005. **38**(15): p. 6533-6543.
19. Barton, A.F., *CRC handbook of solubility parameters and other cohesion parameters*. 1991: CRC PressI Llc.
20. Hansen, C.M., *Hansen solubility parameters: a user's handbook*. 2007: CRC PressI Llc.

국문요약

고분자/클레이 나노복합체는 나노클레이 입자의 넓은 표면적과 높은 종횡비로 인하여 기존 마이크로 사이즈 필러 대비 아주 적은 양의 첨가로도 고분자의 물성을 효과적으로 증대시킬 수 있을 것으로 기대되어 이에 대한 많은 연구가 수행되고 있다. 고분자/클레이 나노복합체의 물성을 발현하기 위해서는 점토입자의 반데르발스 인력으로 적층되어 있는 실리케이트 판상을 박시리키는 과정이 수반되어야 하며, 기존 연구에서 이러한 점토 입자를 박리시키기 위한 방법으로 교류전기장을 조사하는 방법을 소개하였다. 본 연구에서는 이러한 전기장의 효과가 서로 다른 고분자/점토 조합에 따라 다르게 나타나는 것을 확인하여, 향후 전기장을 멜트파이프 등을 이용한 대량생산에 보다 효과적으로 적용하게 할 수 있도록 하기 위하여, 이러한 반응성의 차이를 구체적으로 분석하고 반응성의 차이를 설명하였다. 서로 다른 2가지 고분자로서 비극성인 폴리프로필렌과 상대적으로 극성인 폴리락틱산을 사용하였고, 각각 서로 다른 유기작용기로 치환된 3가지 종류의 클레이를 사용하여 멜트컴파운딩 방법을 통하여 나노복합체를 제조하였다. 전기장은 회전형 레오미터 상에서 개조된 픽스쳐를 사용하여 조사하였고, 이 때 시간에 따른 탄성 모듈러스의 증가, 전기장 조사 전후의 동적 주파수 변조 실험에서 낮은 주파수 영역에서의 탄성 모듈러스의 증가와 말단거동의 사라짐 그리고 투과전자 현미경의 모폴로지를 통하여 전기장의 클레이 입자 박리에 미치는 효과를 확인하였다. 전기장에 대한 반응성의 차이는 고분자/점토 나노복합체의 구조적인 친

화도에 따라 다르게 나타났는데, 비극성인 폴리프로필렌 나노복합체의 경우는 C20A > C10A > C30B의 순서로 반응성이 크게 나타났으며, 상대적으로 극성 고분자인 폴리락틱산 나노복합체의 경우는 이와 반대로 C30B > C10A > C20A의 순으로 반응성이 증가하였다. 전기장에 대한 각각의 나노복합체의 반응성을 정량화하기 위한 방법으로 정상화된 탄성 모듈러스 곡선을 범용 지수증가 함수 식을 이용하여 회귀분석 하였으며 자취를 추적하였다. 이 때, 각 나노복합체의 반응성은 초기에 구조형성이 가파르게 변하는 정도에 따라 달라지는 것을 확인하였고, 이에 반응성의 척도로 곡선의 초기 접선의 기울기를 사용하였다. 전기장의 세기에 따른 초기 접선의 기울기는 폴리프로필렌 나노복합체의 경우 C20A > C10A > C30B의 순서로 나타났고, 폴리락틱산 나노복합체의 경우 C30B > C10A > C20A의 순서로 나타났다. 이러한 결과를 바탕으로 초기 접선의 기울기를 전기장에 대한 반응성을 정량화 하는 파라미터로 사용할 수 있음을 확인하였다. 구조적 관점에서 볼 때, 이러한 전기장에 대한 반응성의 차이는 고분자와 유사한 구조의 유기작용기를 갖는 클레이의 경우 더 높게 나타나는 것을 확인하였으며, 이러한 구조적 유사성을 표현하기 위한 방법으로 한센 용해도 파라미터를 도입하였다. 계산 결과 폴리프로필렌과 C20A, 폴리락틱산과 C30B의 조합이 가장 유사한 한센 파라미터 값을 보였으며, 한센 파라미터 값이 유사할 수록 전기장에 대한 반응성이 더 높은 것을 확인하였으며, 한센 파라미터를 통한 고분자/클레이 간의 친화도의 예측을 통하여 전기장의 효과를 보다 극대화 시킬 수 있을 것으로 보인다.